Journal of Solid State Chemistry 181 (2008) 2804–2807

Contents lists available at ScienceDirect

Journal of Solid State Chemistry

journal homepage: www.elsevier.com/locate/jssc

The direct decomposition of NO over the La_2CuO_4 nanofiber catalyst

Lizhen Gao [a,*], Hui Tong Chua [a], Sibudjing Kawi [b]

[a] School of Mechanical Engineering M050, The University of Western Australia, 35 Stirling Highway, Crawley WA 6009, Australia
[b] Department of Chemical and Biomolecular Engineering, National University of Singapore, 4 Engineering Drive 4, Singapore 117576, Republic of Singapore

ARTICLE INFO

Article history:
Received 16 February 2008
Received in revised form
22 June 2008
Accepted 26 June 2008
Available online 28 June 2008

Keywords:
La_2CuO_4 nanofibers
NO decomposition
Carbon nanotubes
Temperature-programmed desorption

ABSTRACT

The NO catalytic direct decomposition was studied over La_2CuO_4 nanofibers, which were synthesized by using single walled carbon nanotubes (CNTs) as templates under hydrothermal condition. The composition and BET specific surface area of the La_2CuO_4 nanofiber were $La_2Cu^{2+}_{0.88}Cu^{+}_{0.12}O_{3.94}$ and 105.0 m^2/g, respectively. 100% NO conversion (turnover frequency-(TOF): 0.17 $g_{NO}/g_{catalyst}$ s) was obtained over such nanofiber catalyst at temperatures above 300 °C with the products being only N_2 and O_2. In 60 h on stream testing, either at 300 °C or at 800 °C, the nanofiber catalyst still showed high NO conversion efficiency (at 300 °C, 98%, TOF: 0.17 $g_{NO}/g_{catalyst}$ s; at 800 °C, 96%, TOF: 0.16 $g_{NO}/g_{catalyst}$ s). The O_2 and NO temperature programmed desorption (TPD) results indicated that the desorption of oxygen over the nanofibers occurred at 80–190 and 720–900 °C; while NO desorption happened at temperatures of 210–330 °C. NO and O_2 did not competitively adsorb on the nanofiber catalyst. For outstanding the advantage of the nanostate catalyst, the usual La_2CuO_4 bulk powder was also prepared and studied for comparison.

1. Introduction

The exhaust gas from vehicle engines or industrial boilers contains considerable amount of harmful NO, which causes air pollution and acid rain. To remove NO, the selective catalytic reduction (SCR) process using NH_3, CO or hydrocarbon has been applied (three-way catalyst for gasoline fueled vehicles and ammonia SCR for large-scale boilers) [1]. The direct catalytic decomposition of nitric oxide ($2NO = N_2+O_2$) has been considered to be the best technique for NO removal from exhaust streams as NO is thermodynamically unstable relative to the products N_2 and O_2. Because this process eliminates the use of reductants such as CO, NH_3 or hydrocarbon, it will significantly simplify the NO removal technique, decrease the cost and does not create any another pollution [2–6]. Some catalysts, such as copper-ion exchanged ZSM-5 zeolite (Cu-ZSM-5) [7], CeO_2 and Pr_6O_{11} rare earth oxides [8], $La_{1-x}Sr_xMO_{3-\delta}$ (M = Co, Ni, Cu) [9], La(Ba)Mn(In)O_3 perovskite oxides [10], silica-pillared layered titanoniobate supported copper (Cu/Si-$TiNbO_5$) [11], Ag/$La_{0.6}Ce_{0.4}CoO_3$ [12], and supported palladium [13], were active in the direct decomposition of NO. However, most of them only showed good catalytic performance (high NO conversion and high N_2 selectivity) at temperatures higher than 500 °C and were of short catalytic lifetime. Their catalytic performances were insufficient for practical use. The conventional view regarding the low catalytic activity for NO decomposition was that the oxygen in the reaction products strongly competitively adsorbed on the NO active adsorption sites of the catalyst, self-poisoning the catalyst and preventing further NO decomposition [14,15]. For example, the fairly low activities over Pt/Al_2O_3 as well as CuO at 600 °C was because the product O_2 had a strong inhibiting effect and it reacted with un-decomposed NO producing NO_2. So, an effective catalyst for NO decomposition must be active enough to cleave the N–O bond, but the surface-O bond must be weak enough to allow oxygen to desorb at reasonably low temperatures. On the other hand, Cu-ZSM-5 catalyst had poor thermal stability and low tolerance toward H_2O and SO_2 present in exhaust gases; noble metal catalysts had high thermal stability and high tolerance toward H_2O and SO_2 but they were of high cost [16,17]. We have synthesized La_2CuO_4 nanofibers by using single-walled carbon nanotubes as templates under mild hydrothermal conditions [18]. In this paper we report the catalytic performance for NO direct decomposition over such La_2CuO_4 nanofibers. It could catalytically decompose NO completely into nitrogen and oxygen at 300 °C and within 60 h there was a little drop in activity. For outstanding the advantage of the nanostate catalyst, the usual La_2CuO_4 powder was also prepared and studied for comparison.

2. Experimental

Detailed description of the synthesis of La_2CuO_4 nanofibers by using SWNTs as templates was provided in our previous

* Corresponding author. Fax: +61 8 6488 1024.
E-mail address: lizhen@mech.uwa.edu.au (L. Gao).

0022-4596/$ - see front matter © 2008 Elsevier Inc. All rights reserved.
doi:10.1016/j.jssc.2008.06.051

publication [18]. Briefly, the SWNTs were made by cracking of CH_4 ($CH_4/H_2/He = 1/1/8$) at 800 °C over a mixed-oxide catalyst $Mg_{0.8}Mo_{0.05}Ni_{0.10}Co_{0.05}O_x$. The SWNTs sample was purified by nitric-acid washing repeatedly in an ultrasonic bath. The carbon nanotubes were single walled with a 2 nm average inner diameter. For hydrothermal synthesis of La_2CuO_4 single-crystal nanofibers, by using SWNTs as templates, the mixed solution of the surfactant poly(ethylene glycol)-block-poly(propylene glycol)-block-poly (ethylene glycol) (0.1 wt%), $La(NO_3)_3 \cdot 6H_2O$ and $Cu(NO_3)_2 \cdot 6H_2O$ (according to the stoichiometric composition of La_2CuO_4), SWNTs (0.005 wt%) and H_2O_2 (2 mL) was dispersed ultrasonically and was put into an autoclave for hydrothermal synthesis at 60 °C for 20 h. The precipitation obtained from hydrothermal synthesis was filtered and washed with distilled water repeatedly and then was heated at 110 °C for 1 h. Thus La_2CuO_4 nanofibers were synthesized. Roughly, 0.01 g CNTs templates could produce 1 g La_2CuO_4 nanofibers. The CNTs remaining in La_2CuO_4 nanofibers were removed by the method of temperature-programmed oxidation (TPO). We know that carbon nanotubes could be burnt out at temperatures around 650 °C in air [19]. Therefore, the as-synthesized La_2CuO_4 nanofibers were exposed to air at 700 °C for 1 h to remove SWNTs before they were used for catalytic reaction. La_2CuO_4 bulk powder was prepared by heating the mixture of $La(NO_3)_2$ and $Cu(NO_3)_2$ at 800 °C.

The contents of copper in different oxidation states were measured by means of iodometry according to the procedures adopted by Hairis and Hewston [20] and Wu et al. [21]. The oxygen non-stoichiometry values were calculated from the amount of Cu^{2+}, Cu^{+} or Cu^{3+} present, assuming that La^{3+} was in its stable oxidation state.

Oxygen/NO temperature programmed desorption (O_2/NO-TPD) was performed to study O_2/NO adsorption/desorption behaviors. The sample was first exposed to oxygen (or NO) at 150 °C for 2 h for adsorption, and then cooled down to room temperature. The oxygen (or NO) desorbed gradually from room temperature to 800 °C at the rate of 2°/min in the He stream.

The steady-state catalytic activities for NO direct decompositions were measured at atmospheric pressure, 1 h after performance stabilization over a fixed bed quartz micro-reactor. The sample (0.5 g) was placed in the quartz tube between two quartz wool plugs. The quartz tube was placed in a vertical tubular furnace. The total space velocity was 60,000 h^{-1} and the NO feed concentration was 1% with helium being the balance. After steady-state activity was reached, the effluent gas was analyzed by gas chromatography using a molecular sieve 5A column (for the analysis of N_2 and O_2) and a Porapak Q column (for N_2O). The concentration of NO_x ($NO+NO_2$) was monitored with a chemi-luminescence NO_x analyzer. The morphologies of La_2CuO_4 nanofibers and bulk powder were observed under transmission electron microscope (TEM) (JEOL, JEM 2010) and field emission scanning electron microscope (FESEM) (JEOL, JSM 7600F).

3. Results and discussion

The FESEM image of the as-synthesized La_2CuO_4 nanofiber shown in Fig. 1A indicates that the diameter of fibers was around 60 nm and the lengths of fibers were estimated to be nearly 3 μm. After being treated at 700 °C in air, diameter turned to be around 30 nm (Fig. 1B). XRD pattern confirmed that this nanofiber material was of La_2CuO_4 crystal structure [18]. We were not sure whether the nanofibers were hollow tubes or not. The composition and BET-specific surface area of the La_2CuO_4 nanofiber and its bulk powder counterpart were $La_2Cu^{2+}_{0.88}Cu^{+}_{0.12}O_{3.94}$:105.0 and $La_2Cu^{2+}_{0.92}Cu^{3+}_{0.08}O_{4.04}$:2.7 m^2/g, respectively. The BET specific surface areas of Pd-Al_2O_3, Cu-ZSM-5 and Pd/MCM-41 NO decomposition catalysts were about 150 m^2/g [1], 420 m^2/g [14] and 622 m^2/g [4], respectively. The specific surface area of the La_2CuO_4 nanofiber was less than the mesoporous materials but was much higher than the unsupported mixed oxide powders prepared by traditional methods. So far the highest specific area reported for La_2CuO_4 catalyst was 13.0 m^2/g made by sol–gel technique [22]. In the La_2CuO_4 nanofiber there were Cu^{2+}/Cu^{+} and oxygen vacancies while in the bulk powder, there were Cu^{3+}/Cu^{2+} and excess oxygen. The Cu-ZSM-5 was a well known NO decomposition catalyst and has been deeply studied. In Cu-ZSM-5, there were Cu^{+} and Cu^{2+} and when it was exposed to NO, the Cu^{+} ions were oxidized to Cu^{2+}. Whereas the desorption of oxygen could result in the reduction of Cu^{2+} species to the Cu^{+} species, over-exchanged Cu-ZSM-5 showed higher NO decomposition activity and produced more Cu^{+} sites at lower temperatures than the unexchanged sample during the N_2 formation accompanied by the Cu^{+}(NO). Cu^{+} initiated the NO decomposition process. Adsorbed oxygen from dissociated NO changed the oxidation state of Cu^{+} ion, causing the formation of $Cu^{2+}(NO^{3-})$, which decomposed to N_2, N_2O, NO_2 and O_2 [23]. So the existence of the pair of Cu^{+}–Cu^{2+} was the premise for the NO decomposition reaction. Cu^{+} was crucially important for leading the reaction to the products N_2 and O_2. The La_2CuO_4 nanofiber satisfied these requirements. The NO decomposition conversion and the selectivity to each product over the nanofiber and powder La_2CuO_4 catalysts at different temperatures are listed in Tables 1 and 2, respectively. Overall, NO decomposition temperatures over the nanofiber La_2CuO_4 were much lower than those over the usual powder La_2CuO_4 catalyst. 100% NO conversion (turn over frequency-TOF: 0.17 $g_{NO}/g_{catalyst}$ s or 0.17 s^{-1}) was obtained over the nanofiber catalyst at temperatures above 300 °C with products being only N_2 and O_2. When the NO conversion was below 100%, apart from N_2 and O_2, the

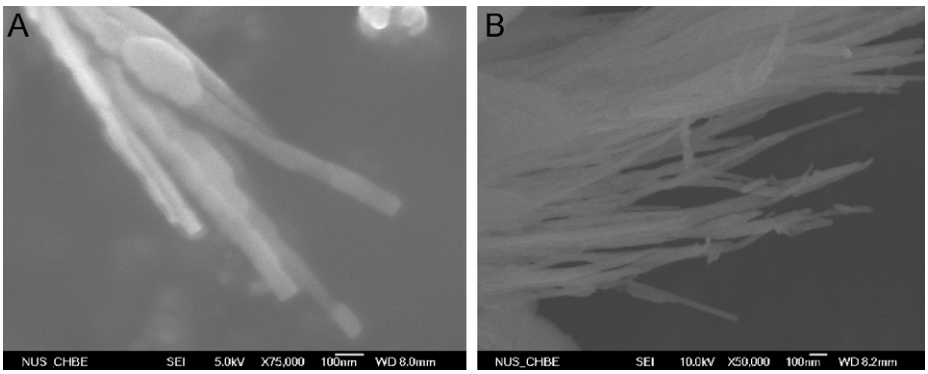

Fig. 1. Field emission scanning electron microscopy (FESEM) images of La_2CuO_4 nanofibers (A): (× 75,000) obtained after hydrothermal synthesis lasting 20 h. (B) (× 50,000) of La_2CuO_4 fiber after being treated in air at 700 °C for 1 h.

Table 1
NO conversions at different temperatures over the La_2CuO_4 nanofiber catalyst

Temperature (°C)	Conversion (%)				
	Of NO	Into N_2	Into O_2	Into N_2O	Into NO_2
100	7.5	4.0	4.1	1.1	2.4
150	19.4	13.5	14.9	2.9	3.0
200	37.9	27.2	27.1	3.5	7.2
250	68.0	59.7	55.6	0.0	8.3
300	100.0	100.0	97.4	0.0	0.0
350	100.0	100.0	98.3	0.0	0.0
400	100.0	100.0	99.0	0.0	0.0
450	100.0	100.0	99.6	0.0	0.0

Table 2
NO conversions at different temperatures over the La_2CuO_4 bulk powder catalyst

Temperature (°C)	Conversion (%)				
	Of NO	Into N_2	Into O_2	Into N_2O	Into NO_2
250	0.0	0.0	0.0	0.0	0.0
300	11.0	6.0	2.4	1.7	3.3
350	12.1	7.2	2.8	1.5	3.4
400	18.5	12.3	4.3	2.1	4.1
450	19.3	13.6	5.1	2.4	3.3
500	21.9	15.7	6.7	2.2	4.0
550	40.4	32.2	9.6	1.7	6.5
600	47.7	36.9	12.9	2.4	8.4
650	58.4	51.3	21.1	1.4	5.7
700	62.0	56.1	28.9	1.2	4.7
750	67.1	58.4	43.3	0.0	8.7
800	78.0	65.8	53.9	0.0	12.2

products consisted of NO_2 and N_2O; O_2 reacted with the undecomposed NO to form NO_2. The oxygen was almost equal to the stoichiometric amount from NO dissociation ($NO = N_2+O_2$; $NO = 1/2N_2O+1/4O_2$; $NO+1/2O_2 = NO_2$), indicating that oxygen weakly adsorbed on the nanofiber catalyst. The temperature around 200–300 °C has met the most practical conditions. For instance, the temperature of automobile exhaust was between 200 and 300 °C [24]. Over the bulk La_2CuO_4 powder, only 78% NO was decomposed (TOF: $0.13\,s^{-1}$) even at the high temperature of 800 °C with the products being N_2, O_2, and NO_2. When the temperature was less than 700 °C, the product included N_2O. The oxygen measured was much less than the stoichiometric amount from NO dissociation, suggesting that oxygen strongly adsorbed on the powder catalyst. The catalytic activity durability (at 300 and 800 °C) over both the La_2CuO_4 nanofiber and powder catalysts has been tested and the results are shown in Fig. 2. In 60 h on stream testing, either at 300 °C or at 800 °C, the nanofiber catalyst showed high NO conversion (at 300 °C, 98%, TOF: $0.17\,s^{-1}$; at 800 °C, 96%, TOF: $0.16\,s^{-1}$) with a slight drop. Hence, improving its stability was a task for practical application. It was found that after 60 h on stream test, the content of Cu^+ decreased a little in the nanofibers ($La_2Cu^{2+}_{0.90}Cu^{+}_{0.10}O_{3.94}$). Over the bulk powder catalyst, at 300 °C, NO conversion dropped a little and remained 11% (TOF: $0.019\,s^{-1}$) while at 800 °C, it dramatically decreased from 78 to 18% ($0.031\,s^{-1}$). These results indicated that the nanofiber was of higher thermal stability than the bulk powder. Zhu et al reported that at 850 °C over $LaSrCuO_4$ and La_2CuO_4 catalysts NO (NO 1%, flow rate 22.3 ml/min, 0.5 g catalyst) conversion values were 34.3% (TOF: $3.43\times10^{-6}\,s^{-1}$) and 4% (TOF: $4.0\times10^{-7}\,s^{-1}$), respectively [25]. Over the Cu-ZSM-5 catalyst, at 550 °C the conversion of NO, and of conversion into N_2 and O_2 were 97%, 85%, and 70%, respectively (contact time: $10.0\,g\,s\,cm^{-3}$) [17]. Over Pd/Al_2O_3/MCM-41 and at 450 °C , the initial NO conversion reached 100% (500 ppm NO, 120 ml/min, 30,000 h^{-1}, TOF: $4\times10^{-3}\,s^{-1}$), but when the reaction time lasted for about 250 min, the NO conversion dropped to less than 10% (TOF: $4\times10^{-4}\,s^{-1}$). The products were N_2, O_2 and N_2O. The quick removal of the surface oxygen was a crucial requirement to this catalyst [4]. Amongst the perovskite-type mixed oxide catalysts La–Sr–Ni–Co, La–Sr–Mn–Co, La–Sr–Mn–Ni, La–Sr–Ag–Ni, La–Sr–Cu–Fe, La–Sr–Ti–Cu, La–Sr–Ni–Co–Fe, La–Sr–Cu–Al, La_2CuO_4/CuO/$LaFeO_3$, at 680 °C, NO conversion was less than 20% (5% NO in He, 50 ml/min, 1 g catalyst, TOF: $1.12\times10^{-5}\,s^{-1}$) [9]. Over Pd/Al_2O_3 and $Pd–Mo/Al_2O_3$ catalysts, at 400 °C, at the beginning, NO conversion reached 100% (SV 4×10^4 mol of feed/h. mol Pd; TOF: $3.14\,g.s^{-1}$/g Pd); but after 2 h, it dropped to about 50% (TOF: $3.14\,g.s^{-1}$/g Pd) [5]. Amongst the series of perovskite catalysts La–Ba–Cr–Ga, La–Ba–Fe–Ca, La–Ba–Cu–Ca, La–Ba–Co–Ga, La–Sr–Mn–In, La–Ca–Mn–In, La–Ba–Mn–Ca and La–Ba–Mn–Al, $La_{0.7}Ba_{0.3}Mn_{0.8}In_{0.2}O_3$ showed the highest activity: at 800 °C (1 g catalyst, 1.0% NO, $W/F = 3.0\,g\,s\,cm^{-3}$), NO conversion was 96.8% (TOF: $4.3\times10^{-6}\,s^{-1}$; 63.7% into N_2 33.1% into NO_2) and almost no activity drop in 700 min [10]. Over Pd/Al_2O_3 by using Pd $(CH_3COO)_2$ as precursor, at 800 °C, N_2 formation rate was 3.5 mol $min^{-1}\,g^{-1}\times10^{-6}$ (TOF: $1.25\times10^{-6}\,s^{-1}$).[1]Over Pd/Al_2O_3, at 500 °C (1000 ppm NO, flow rate = 30 ml/min, $W/F = 1.0\,g\,s\,cm^{-3}$), 20% of NO was decomposed to N_2 (TOF: $3\times10^{-4}\,s^{-1}$) [2]; at 900 °C, the conversion climbed up to 80% (TOF: $1.2\times10^{-3}\,s^{-1}$) [2]. The catalytic efficiency of La_2CuO_4 nanofiber was higher than of most of the reported catalysts.

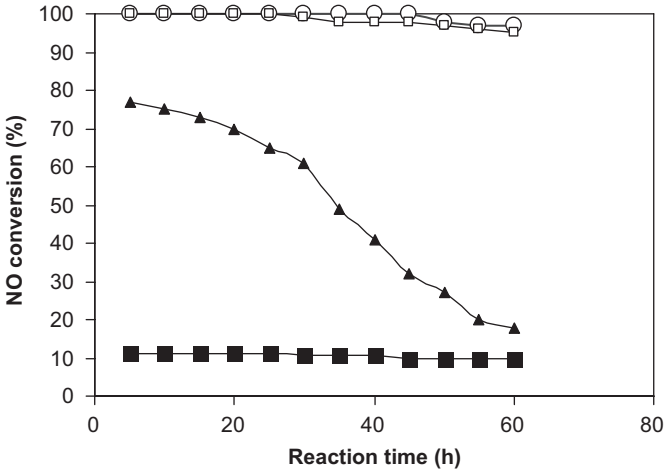

Fig. 2. The plots of NO conversion vs reaction time over the La_2CuO_4 nanofiber at 300 °C (○) and 800 °C (□) and La_2CuO_4 bulk powder at 300 °C (▲) and 800 °C (■).

The TPD curves of oxygen desorption (O_2-TPD) over the La_2CuO_4 nanofiber and bulk powder are shown in Fig. 3A. There were two oxygen desorption peaks over the nanofiber catalyst at the temperature ranges 80–190 and 720–900 °C. Over the bulk powder catalyst, oxygen desorption occurred at temperatures 500–610 °C and above 870 °C. This result indicated that the desorption of oxygen over the nanofiber was easier than over the bulk powder. The oxygen vacancies existing in nanofiber might help the release of oxygen at low temperature. The NO-TPD results shown in Fig. 3B indicate that over the nanofiber catalyst, NO desorption occurred at temperatures 210–330 °C and over the bulk powder it happened at 500–620 °C, suggesting that at lower temperature NO was more active over the nanofiber than over the bulk powder. Over the nanofiber catalyst, NO and O_2 did not release at the same temperature region while over the bulk powder they did. We speculated that over the bulk powder NO and O_2 adsorbed competitively while over the nanofiber they did not. The O_2 desorption over the Cu-ZSM-5 catalyst occurred at temperatures 130 and 530 °C; NO desorption occurred at

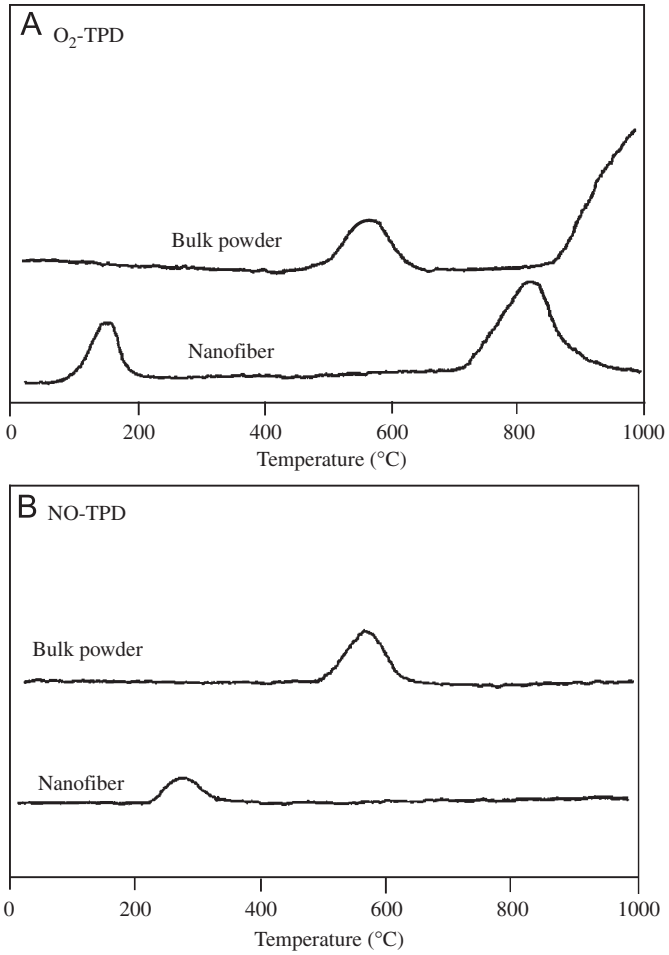

Fig. 3. O_2 (A) and NO (B) temperature programmed desorption (TPD) curves over the La_2CuO_4 nanofiber and bulk powder catalysts.

temperatures 130–330 °C; NO and O_2 adsorbed competitively [15]. Promotion of oxygen desorption at low temperature held the key to the development of an NO decomposition catalyst. Addition of Tb oxide to Pt/Al_2O_3 allowed oxygen from dissociated NO to desorb at 320 °C, which was significantly lower than the reported oxygen desorption temperature over Pt catalyst. The Tb addition significantly enhanced the NO decomposition activity (measured by pulsing method; NO conversion: 12–28%) [6]. The nanoscale materials were expected to be potential catalyst in future chemical engineering. But so far, most of the nanomaterials were in powder particles, which were of disadvantages in pressure drop, heat/mass transfer and separation processes. The fiber nanofiber catalysts may avoid these problems. The $LaMnO_3$ perovskite nanofiber catalyst has been synthesized by using carbon nanotubes as templates and showed higher catalytic activity for propane oxidation than the $LaMnO_3$ powder catalyst [26].

In summary, La_2CuO_4 nanofiber was a promising NO remove catalyst owing to its special structure, high specific area, appropriate Cu^+/Cu^{2+} ratio and uncompetitive O_2 and NO adsorptions. Its longevity still needs to be prolonged.

Acknowledgment

We gratefully acknowledge the financial support under an A*STAR SERC Grant (A*STAR project no: 0221010035).

References

[1] M. Haneda, Y. Kintaichi, I. Nakamura, T. Fujitani, H. Hamada, J. Catal. 218 (2003) 405.
[2] M. Haneda, Y. Kintaichi, I. Nakamura, T. Fujitani, H. Hamada, Chem. Commun. (2002) 2816.
[3] F. Garin, Appl. Catal. A 222 (2001) 183.
[4] J.M.D. Cónsul, C.A. Peralta, E.V. Benvenutti, J.A.C. Ruiz, Heloise O. Pastore, I.M. Baibich, J. Mol. Catal. A 246 (2006) 33.
[5] G.M. Tonetto, M.L. Ferreira, D.E. Damiani, J. Mol. Catal. A 193 (2003) 121.
[6] Steven S.C. Chuang, C.D. Tan, J. Phys. Chem. B 101 (1997) 3000.
[7] V.I. Parvulescu, M.A. Centeno, P. Grange, B. Delmon, J. Catal. 191 (2000) 445.
[8] M. Haneda, Y. Kintaichi, H. Hamada, Phys. Chem. Chem. Phys. 4 (2002) 3146.
[9] C. Tofan, D. Klvana, J. Kirchnerova, Appl. Catal. A 223 (2002) 275.
[10] T. Ishihara, M. Ando, K. Sada, K. Takiishi, K. Yamada, H. Nishiguchi, Y. Takita, J. Catal. 220 (2003) 104.
[11] X. Wang, W. Hou, X. Wang, Q. Yan, Appl. Catal. B 35 (2002) 185.
[12] Z. Liu, J. Hao, L. Fu, T. Zhu, Appl. Catal. B 44 (2003) 355.
[13] S. Naito, M. Iwahashi, I. Kawakami, T. Miyao, Catal. Today 73 (2002) 355.
[14] A. Gervasini, Appl. Catal. B 14 (1997) 147.
[15] Y. Li, W.K. Hall, J. Phys. Chem. 94 (1990) 6145.
[16] M. Iwamoto, H. Furukawa, Y. Mine, F. Uemura, S. Mikuriya, S. Kagawa, J. Chem. Soc., Chem. Commun. (1986) 1272.
[17] M. Iwamoto, H. Hamada, Catal. Today 10 (1991) 57.
[18] L.Z. Gao, X.L. Wang, H.T. Chua, S. Kawi, J. Solid State Chem. 179 (2006) 2036.
[19] B.C. Liu, L.Z. Gao, Q. Liang, S.H. Tang, M.Z. Qu, Z.L. Yu, Catal. Lett. 71 (2001) 225.
[20] D.C. Hairis, T.A. Hewston, J. Solid State Chem. 69 (1987) 182.
[21] Y. Wu, Z. Zhao, Y. Liu, X. Yang, J. Mol. Catal. A 155 (2000) 89.
[22] M.J. Akhtar, C.R.A. Catlow, S.M. Clark, W.M. Temmerman, J. Phys. C 21 (1988) L917.
[23] Mahesh V. Konduru, Steven S.C. Chuang, J. Phys. Chem. B 103 (1999) 5802.
[24] I. Melián-Cabrera, C. Mentruit, J.A.Z. Pieterse, R.W. van den Brink, G. Mul, F. Kapteijn, J.A. Moulijn, Catal. Commun. 6 (2005) 301.
[25] J. Zhu, Z. Zhao, D. Xiao, J. Li, X. Yang, Y. Wu, Ind. Eng. Chem. Res. 44 (2005) 4227.
[26] H. Ogihara, M. Sadakane, Q. Wu, Y. Nodasaka, W. Ueda, Chem. Commun. (2007) 4047.